Chemistry of Triple-Decker Sandwich Complexes Containing Four-Membered Open B2E2 Rings (E = S or Se)

B. Joseph, S.K. Barik, R. Ramalakshmi, G. Kundu, T. Roisnel, V. Dorcet, S. Ghosh

Chemistry of Triple-Decker Sandwich Complexes Containing Four-Membered Open B_2E_2 Ring (E = S or Se)

Benson Joseph,[a] Subrat Kumar Barik,†[a] Rongala Ramalakshmi,†[a] Gargi Kundu,[a] Thierry Roisnel,[b] Vincent Dorcet,[b] and Sundargopal Ghosh*[a]

Abstract: Building upon our earlier studies on cobaltaheteroboranes, we explored the chemistry with heavier group 9 metals. Reaction of $[Cp^*M(\mu\text{-}Cl)Cl_x]_2$ ($Cp^* = \eta^5\text{-}C_5Me_5$; M = Co, x = 0; M = Rh or Ir, x = 1) with $[LiBH_4{\cdot}THF]$ followed by thermolysis with excess of chalcogen powders (S or Se) afforded dimetallaheteroboranes *nido*-$[(Cp^*M)_2B_2H_2E_2]$, **1**-**4** (**1**: E = S, **2**: E = Se, M = Co; **3**-**4**: E = Se, M = Rh and Ir) in moderate to good yields. The solid state X-ray structures of these compounds show open-cage triple decker clusters. Attempts to isolate the Te analogue was failed, however, in case of cobalt, we have isolated an 11 sep *nido*-$[(Cp^*Co)_2B_5H_5Te_2]$, **5**. The X-ray structure of **5** shows mono-capped square antiprism geometry having two Te atoms in the core. In order to close the central four-membered B_2E_2 open ring of *nido*-**1** and *nido*-**2**, we have performed the reaction with $[Ru_3(CO)_{12}]$ that led to the formation of *closo*-$[(Cp^*Co)\{\mu\text{-}\eta^5\text{:}\eta^5\text{-}B_2H_2E_2M\}M\{\mu\text{-}Ru(CO)_4\}]$, **6**-**7** (**6**: E = S, **7**: E = Se; M = $Ru(CO)_2$). In contrast, the reactions of *nido*-**2** and *nido*-**3** with $[Fe_2(CO)_9]$ resulted heterometallic clusters *nido*-$[(Cp^*M)Fe(CO)_3B_2H_2Se_2]$, **8**-**9** (**8**: M = Co; **9**: M = Rh), $[(Cp^*Co)Fe_3(CO)_8Se_2]$, **10** and $[(Cp^*Co)Fe_2(CO)_7Se]$, **11**. As *nido*-**8** also contains a four-membered open ring B_2Se_2, we treated this with $[Ru_3(CO)_{12}]$ that yielded *closo*-$[(Cp^*Co)\{\mu\text{-}\eta^5\text{:}\eta^5\text{-}B_2H_2Se_2M\}M\{\mu\text{-}Fe(CO)_4\}]$, **12** (M = $Ru(CO)_2$), analogous to that of **7**. In addition, we have analyzed the divergence in reactivity of *nido*-$[(Cp^*M)_2B_2H_2E_2]$, **2**-**4** with the help of density functional theory (DFT) calculations.

Introduction

The chemistry of metallaheteroboranes traditionally achieved by the reaction of polyhedral heteroborane anions with metal fragments or the incorporation of heteroatom into metallaborane clusters.[1-5] The developments towards the large numbers of metallaheteroborane have gained pronounced deal of interest owing to their utility in the preparation of high-nuclearity clusters.[6] Among them, group 9 metallaheteroboranes have received significant attention due to their applications in catalysis.[7-8] For example, *nido*-rhodathiaborane [8,8,8-$(PPh_3)_2$H-9-(NC_5H_5)-*nido*-8,7-$RhSB_9H_9$] acts as a catalyst for the isomerization and hydrogenation of alkenes.[8c] Although, metallaheteroboranes comprised of thia[3,4,7,8] and aza[4b] ligands have been explored, compounds that contain heavier heteroatoms such as selenolato[9] and tellurolato[10] ligands are relatively limited. As a result, we[5a-c,11] and others[6-10] have synthesized interesting metallaheteroborane clusters containing selenium and tellurium that illustrate different reactivity and structural patterns as compared to sulfide clusters.[12]

In the past several years, we have been actively involved in the synthesis of metallaheteroboranes containing heavier chalcogen atoms that enabled us to synthesize a series of group 5,[11b,13] 6[5c-e,11c,12a-b,14] and 8[5a-b,15] metallaheteroboranes through the activation of diorganyldichalcogenide ligands or chalcogen powders. For example, group 6 dimetallaheteroboranes $[(Cp^*Mo)_2B_4H_{5+m}Cl_nE]$[11c,12a] (E = Te, m = 0, n = 1; E = S or Se, m = 1, n = 0) show diverse reactivity patterns towards many metal carbonyls yielding metallaheteroboranes containing six-membered middle ring.[14d,16] Grimes reported the first neutral and air stable cobalt triple decker compounds $[(CpCo)_2RC_2B_3H_4]$ (R = Me/H), inclosing a central $[RC_2B_3H_4]_4$ ring.[17] Recently, we have also reported various triple-decker compounds $[(Cp^*Mo)_2\{\mu\text{-}\eta^6\text{:}\eta^6\text{-}B_4H_4ERu(CO)_3\}]$ from the reaction of $[(Cp^*Mo)_2B_4H_6E]$ (E = S and Se) and $[Ru_3(CO)_{12}]$.[16] Synthesis of $[(CpCo)_2B_2H_2S_2]$ by Sneddon[18] and our recent studies on $[(Cp^*Co)_2B_2H_2E_2]$ (**1**: E = S; **2**: E: Se)[19,20] led us to explore the chemistry of heavier group 9 metals. Thus, analogous the rhodium and iridium systems became of interest. In this report, we describe the synthesis and chemistry of group 9 triple decker sandwich metallaheteroboranes containing four-membered open B_2E_2 central ring (E = S or Se).

Results and Discussion

Syntheses of group 9 open cage triple decker compounds

As shown in Scheme 1, the reaction of $[Cp^*M(\mu\text{-}Cl)Cl]_2$ (M = Rh or Ir) and $[LiBH_4{\cdot}THF]$ followed by thermolysis in presence of Se powder yielded corresponding dimetallaheteroboranes *nido*-$[(Cp^*M)_2B_2H_2Se_2]$, (**3**: M = Rh, **4**: M = Ir) in moderate yields.[21] The identity of these dimetallaheteroboranes was unambiguously established by multinuclear NMR spectroscopy, HR-MS, FT-IR, X-ray crystallography and computational analysis (DFT). The $^{11}B\{^1H\}$ NMR spectrum of **3** reveals a sharp signal at δ = 23.9 ppm which is downfield shifted as compared to **4** (δ = 7.3 ppm) but upfield shifted as compared to **1** (δ = 33.5 ppm). The $^1H\{^{11}B\}$ spectra of **3** and **4** display resonaces at δ = 4.50 and 2.98 ppm respectively for B-H_t. Further, the $^1H\{^{11}B\}$ and $^{13}C\{^1H\}$ NMR support the presence Cp* ligand. The mass

[a] B. Joseph, Dr. S. K. Barik, R. Ramalakshmi, G. Kundu, Prof. Dr. S. Ghosh
Department of Chemistry
Indian Institute of Technology Madras, Chennai 600036, India
E-mail: sghosh@iitm.ac.in
Homepage: http://chem.iitm.ac.in/faculty/sundargopalghosh/
[b] Dr. T. Roisnel, V. Dorcet
Institut des Sciences Chimiques de Rennes, UMR 6226 CNRS-Ecole Nationale Supérieure de Chimie de Rennes-Université de Rennes 1, F-35042 Rennes Cedex, France.
† These authors contributed equally to this work.
Supporting information for this article is given via a link at the end of the document.

spectra of **3** and **4** show molecular ion peaks (ESI^+) at *m/z* 682.8986 and 841.0363 respectively. These spectroscopic data validate the existence of C_2 symmetry in these molecules.

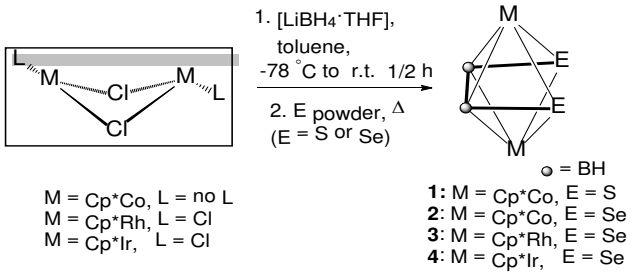

Scheme 1. Synthesis of open cage triple decker metallaheteroboranes of group 9 metals.

Single crystals of **3** and **4** suitable for analysis were obtained from the hexane/CH_2Cl_2 solution at 3 °C. By changing the metal to heavier metal Ir, compound **4** crystallized in C2/*c* space group rather than $P2_1/c$. The solid state structures of **3** and **4** represents an open-cage triple decker in which two metals are sandwiched between the open [B_2Se_2] ring and two Cp* ligands (Figure 1). The vertical mirror plane along the C_2 axis, bisects the B1-B2 bond which provides a C_{2v} symmetry in the molecule. Alternatively, this geometry can be described as pentagonal bipyramid, in which one of the atoms is missing at the equatorial plane. According to the Wade-Mingos electron counting rule,[22] this *nido* open-cage geometry consistent with 8 sep, [2(Cp*M) X 2 + 2(μ_3-Se) X 4 + 2(BH) X 2 /2] (M = Rh or Ir). As shown in Figure 1, overall the structures of **3** and **4** are similar to that of

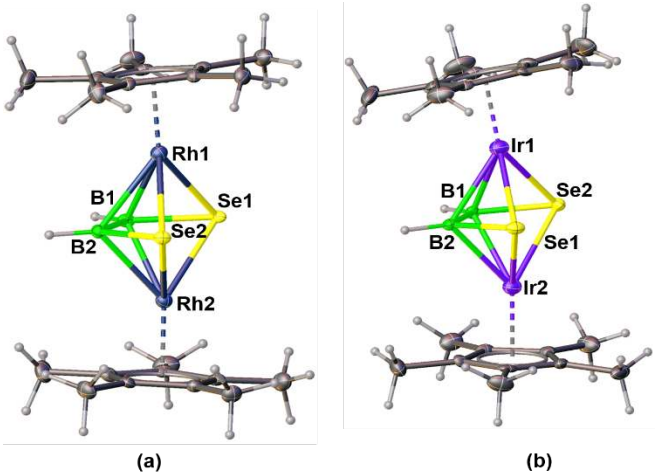

Figure 1. (a) Molecular structures of **3** and **4**. Selected bond lengths (Å) and angles (°): **(a)** Rh1-B1 2.231(3), Rh1-B2 2.237(3), Rh1-Se1 2.5031(4), Rh2-B1 2.226(3), Rh2-B2 2.230(3), Rh2-Se1 2.5038(4), B1-Se1 1.983(3), B2-Se2 1.980(3), B1-B2 1.739(4), Rh1-B1-Rh2 100.08(11), Rh1-B2-Rh2 99.78(11), Rh1-Se1-Rh2 86.046(13), Rh1-Se2-Rh2 86.270(11); **(b)**: Ir1-B1 2.217(7), Ir1-B2 2.211(8), Ir2-B1 2.235(7), Ir2-B2 2.226(6), Ir1-Se1 2.5053(7), Ir2-Se1 2.5026(7), B1-Se2 1.998(8), B2-Se1 1.985(7), B1-B2 1.746(10), Ir1-B1-Ir2 102.2(3), Ir1-B2-Ir2 102.7(3), Ir1-Se1-Ir2 87.55(2), Ir1-Se2-Ir2 87.31(2).

$[(Cp^*Co)_2B_2H_2Se_2]$[20]. The two Ir atoms in **4** are separated by 3.465 Å, which is comparatively longer as compared to Rh-Rh (3.416 Å) and Co-Co (3.144 Å) distances. Similarly the B-Se distance of 1.998(8) Å in **4** is relatively longer as compared to **3** (1.983(3) Å) and **2** (1.985(6) Å). Although the B1-B2 distances of 1.746(10) Å for **4** and 1.739(4) Å for **3** fall within the standard range,[20,23] the M-B (M = Rh or Ir) bond lengths are comparatively shorter as compared to those of related metallaborane clusters.[23b-d]

Density functional theory (DFT) calculations were used to probe the reactivity patterns of **2**-**4** at the PBE0/Def2-TZVP level of theory. The bond lengths and the NMR chemical shift values of **2**-**4** closely matched with those of the experimental values (Tables S1 and S2). The molecular orbital study of **2**-**4** shows that the HOMO-LUMO energy gap increases in the order of **2**<**3**<**4** (Figure 2, Table S3) which is consistent with their thermodynamic stability. In addition, a significant destabilization of HOMO of **2**, suggests a higher reactivity compared to **3** and **4**. Inspection of electron density of the FMOs of **2**-**4** reveals that HOMOs are predominantly localized on metal and Se atoms. Further, the shapes of HOMO-3 and LUMO+3 of **2**-**4** disclose the bonding and anti-bonding interactions between the boron and metal centers (Figure S30). The B-B and M-Se Wiberg bond indices for **2**-**4** were found to be close to 0.7 and 1.04 respectively in all cases. However, the M-M Wiberg bond indices for **2**-**4** were close to 0.07 that indicate absence of bonding interaction between two metal centers (Table S4).

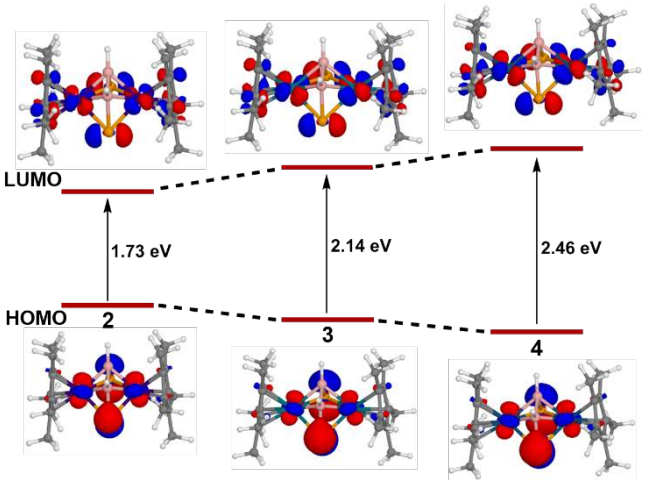

Figure 2. Frontier molecular orbital diagram of **2**-**4** (contour value: ±0.05 $[e/bohr^3]^{1/2}$).

Examples of metallaheteroborane clusters with heavier group 16 elements, especially Te atom are limited.[14d,16] Thus, to isolate tellurium analogue of *nido*-**1**, we have performed the reaction of $[Cp^*CoCl]_2$ and [$LiBH_4$·THF] followed by thermolysis with Te powder. In contrast to the earlier results, this reaction led to the formation of a *nido*-$[(Cp^*Co)_2B_5H_5Te_2]$, **5** and $[(Cp^*Co)_2B_4H_6]$[24] (Scheme 2). All of our attempts to isolate the Rh and Ir analogues of **5** were failed. The reaction yielded all known clusters, such as $[(Cp^*Rh)_2B_3H_7]$[25] and $[Cp^*IrH_4]$[26] in low

yields respectively. Compound **5** was isolated as violet crystals and characterized by the NMR spectroscopy, mass spectrometry, X-ray diffraction and DFT studies.

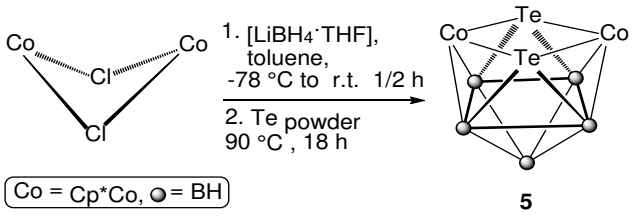

Scheme 2. Synthesis of cluster **5**.

Compound **5** crystallizes in monoclinic *C*2/*c* space group in which the asymmetric unit consists of two Co atoms each ligated to Cp* ligand, two B-H units and two μ_4-Te atoms. The molecular structure of **5**, shown in Figure 3, shows that the cage geometry is mono-capped square antiprism comparable to that of $[Ni_9C(CO)_{17}]^{2-}$[27] having an interstitial carbon atom at the center. According to the cluster electron-counting rules,[22] compound **5** possesses 11 skeletal electron pairs (sep) [2(Cp*Co) × 2 + 4(μ_4-Te) ×2 + 2(BH) × 5)}/2] and thus it obeys Wade rules. Cluster **5** has C_{2v} symmetry with two Co and two Te atoms in the open cage. Among the five boron atoms, one of the boron atoms is capped by four other boron atoms, which is in a plane of the mono-capped square antiprism. The molecule has no direct Co-Co ($d_{Co\text{-}Co}$ 3.645 Å) and Te-Te ($d_{Te\text{-}Te}$ 3.406 Å) bonds (Figure 3). Although the B-B and Co-B bond distances fall in the range observed for other characterized cobaltaboranes,[19,20,24] the Co-Te bond distance of 2.5019(6) Å is marginally shorter than the corresponding single bond that ranges between 2.575(5)-2.614(5) Å.[28] The B-Te bond distance of 2.347(5) Å is significantly longer as compared to other telluraboranes, e.g., $[(CpMo)_2B_4H_4Te_2]$ ($d_{B\text{-}Te}$ = 2.033(11)[14a] and 2.299(13) Å) and

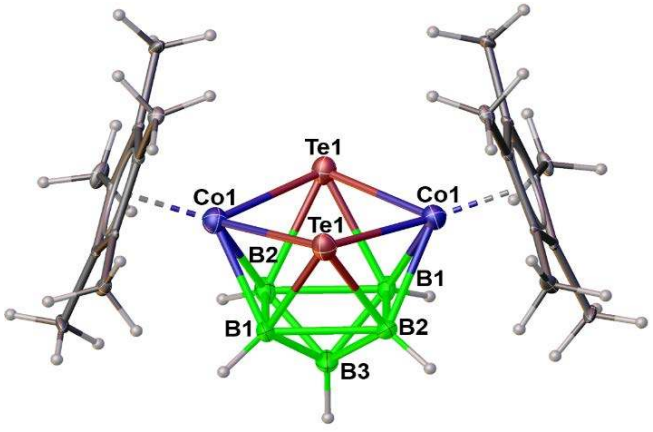

Figure 3. Molecular structure of **5**. Selected bond lengths (Å) and angles (º): Co1-Te1 2.5019(6), Te1-B1 2.347(5), Te1-B2 2.347(5), Co1-B1 2.154(5), Co1-B2 2.149(5), B1-B2 1.824(8), B2-B1 2.015(6), B1-B3 1.680(6), B3-B2 1.680(6), B(1)-Co(1)-Te(1) 94.42(14), B(1)-Te(1)-B(2) 50.85(16), B(1)-B(3)-B(2) 73.7(3).

$[(Cp^*Mo)_2\{\mu\text{-}\eta^6\text{:}\eta^6\text{-}B_3H_3TeCo_2(CO)_5\}]$ ($d_{B\text{-}Te}$ = 2.238(7) Å).[14d]

Consistent with the solid state X-ray structure determination, the room temperature $^{11}B\{^1H\}$ NMR spectrum reveals two types of boron chemical shifts at δ = -3.6 and -8.5 ppm in 4:1 ratio. The $^1H\{^{11}B\}$ NMR spectrum shows two singlet peaks that correspond to two types of B–H terminal protons appeared at δ = 6.00 and 2.96 ppm. The combination of $^1H\{^{11}B\}$ NMR and $^{13}C\{^1H\}$ NMR spectra infer the presence of Cp* ligand. These spectroscopic data also reflects the presence of symmetry in the molecule.

To gain insight into the electronic structure and bonding of **5**, we have carried out geometry optimization of **5'** (Cp analogue of **5**) by DFT methods (Figures 4a-b). The calculated Co1-Co1 and Te1-Te1 distances of 3.638 and 3.442 Å respectively are in good agreement with the experimental data obtained from the solid state X-ray structure ($d_{Co1\text{-}Co1}$ = 3.645 and $d_{Te1\text{-}Te1}$ = 3.406 Å). Accordingly, the computed distance of 2.321 Å for B1-Te1 bond is very close to the experimental data of 2.347(5) Å. The topological analysis of the electron density of Co1-Te1-Co1-Te1 plane indicates the occurance of BCPs along the Co-Te bond paths (Figure 4c). As expected, no BCPs were observed for Co1-Co1 and Te1-Te1 atom pairs indicating **5'** with no direct bonds between two Co atoms and two Te atoms. Thus, compound **5** unveils a *nido* cluster that can be accessed from a 10 vertex bicapped square antiprism by removing one of the capped vertices.

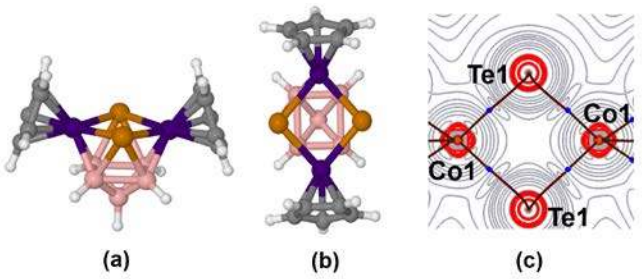

Figure 4. (a) and (b) Illustration of optimized geometry of **5'** in different orientations, (c): Contour line diagrams of the Laplacian of the electron density, $\nabla^2\rho(r)$ of Co1-Te1-Co1-Te1 in **5'** that generated using the Multiwfn program package at the PBE0/Def2-TZVP level of theory.

Reactivity of *nido*-1 and *nido*-2 with $[Ru_3(CO)_{12}]$

Earlier, Fehlner and co-workers have demonstrated that the central open ring of $[(Cp^*Re)_2B_4H_8]$[29] can be closed if this is treated with $[BHCl_2.SMe_2]$ or $[Co_2(CO)_8]$. The reactions led to the formation of triple-decker complexes $[(Cp^*Re)_2\{\mu\text{-}\eta^6\text{:}\eta^6\text{-}B_6H_4Cl_2\}]$[30] and $[(Cp^*Re)_2\{\mu\text{-}\eta^6\text{:}\eta^6\text{-}B_4H_4Co_2(CO)_5\}]$[31] respectively that contain six-membered ring as the middle-deck. In a similar fashion, Barton has synthesized *closo*-$[B_5H_4PPh_3\{Fe(CO)_3\}\{Ir(CO)_2PPh_3\}]$ from the reaction of *nido*-$[B_5H_8\{Ir(CO)(PPh_3)_2\}]$ and $[Fe_2(CO)_9]$.[32] Therefore, we planned to close the central open ring of *nido*-**1** and *nido*-**2** by reacting them with $[Ru_3(CO)_{12}]$. The reactions indeed led to the formation of *closo*-$[(Cp^*Co)\{\mu\text{-}\eta^5\text{:}\eta^5\text{-}B_2H_2E_2\text{-}Ru(CO)_2\}Ru(CO)_2\{\mu\text{-}Ru(CO)_4\}]$,

(**6**: E = S and **7**: E = Se) (Scheme 3). The $^{11}B\{^1H\}$ NMR spectra show the presence of one type of resonance for **6** (δ = 19.9 ppm) and **7** (δ = 22.3 ppm). The $^1H\{^{11}B\}$ NMR spectra of **6** and **7** displayed one type of Cp* protons along with one type of terminal B-H protons. The presence of Cp* ligand has also been supported by $^{13}C\{^1H\}$ NMR. Further, the mass spectra of **6** and **7** show molecular ion peaks (ESI^+) at *m/z* = 812.7104 and 930.5797 respectively. The IR spectra show strong absorption bands at 1997, 1934 cm^{-1} for **6** and 2002, 1924 cm^{-1} for **7** that correspond to terminal carbonyl groups.

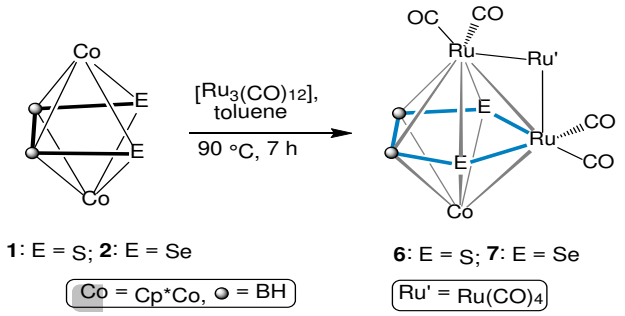

Scheme 3. Synthesis of seven vertex *closo*-**6** and *closo*-**7**.

In order to confirm the spectroscopic assignments and to define the solid state X-ray structure, an X-ray structure analysis was undertaken. The solid-state structure of **7**, shown in Figure 5a, is consistent with the spectroscopic data. The core geometry of **7** is pentagonal bipyramid in which one *exo*-polyhedral $Ru(CO)_4$ moiety is bonded with two Ru atoms of **7** (Figure 5a). The molecule possesses a planer five-membered $\{B_2Se_2Ru\}$ ring, which is sandwiched between Cp*Co and $[Ru(CO)_2\{\mu\text{-}Ru(CO)_4\}]$ moeties (the mean plane deviation is 0.18 Å and sum of internal angles 539.25°). Within the ring, the B-B distance of 1.673(7) Å is shorter as compared to *nido*-**2** ($d_{B\text{-}B}$ = 1.726(7) Å.[20]

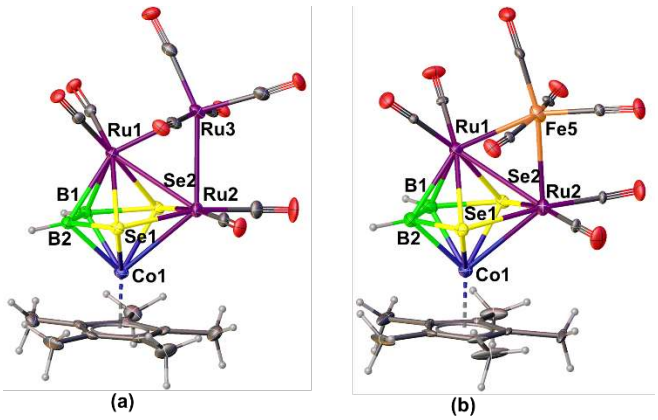

Figure 5. Molecular structures of **7** and **12**. Selected bond lengths (Å) and angles (º): **(a)** Ru1-Ru2 2.911(5), Ru1-Ru3 2.776(5), Co1-B1 2.151(5), Co1-Se1 2.4143 (7), Ru2-Se2 2.526(6), Ru1-B1 2.299(5), Se2-B1 2.032(5), B1-B2 1.673(7), B2-B1-Se2 116.9(3), Ru1-Ru3-Ru2 63.423(12); **(b)**: Ru1-Fe5 2.7198(8), Ru2-Fe5 2.6739(9), Co1-B1 2.152(6), Co1-Se1 2.3966(7), Co1-Se2 2.4058(8), Ru2-Se1 2.5183(6), Ru1-B1 2.301(6), Se2-B1 2.010(6), B1-B2 1.647(9); B2-B1-Se2 117.9(4), Ru1-Fe5-Ru2 64.63(2).

Compound **7** features a triangular trimetallic unit (Ru1-Ru2-Ru3) connected to the parent pentagon $[Ru_2B_2Se_2Co]$ by means of Ru1-Ru2 bond {∠Ru1-Ru3-Ru2 = 63.423(12), ∠Ru1-Ru2-Ru3 = 58.522(12), ∠Ru2-Ru1-Ru3 = 58.055(12)}. Alternatively, compound **7** may be considered as a fused cluster generated by the condensation of *closo*-$[(Cp^*Co)B_2Se_2Ru_2(CO)_4]$ (pentagonal bipyramid) and $\{Ru_3(CO)_8\}$ (triangle) through a common Ru-Ru bond. Total valence electron counts of 74 can be described by Mingos fusion formalism.[22] The total valence electron pair (TVEP) for this molecule can also be described using Jemmis *mno* rule[33]. The *mno* rule gives m = 2, n = 12 and o = 1, p = 1, x = 4, x_s = 1, n_s = 1, for $m + n + o + p + 6x - x_s/n_s\{3(m - 1)\} = 37$ electron pairs, e. g., 74 cluster valence electrons (where m = number of polyhedra, n = number of vertices in the fused cluster, o = number of single vertex shared atoms, p = number of missing vertices, x = number of transition metals, x_s = number of shared transition metals and n_s = number of shared atoms).

To provide further insight into the bonding situation of the central ring of **7**, the DFT calculations were carried out. Although the experimental bond distances of Ru2–Se1 and Ru2-Se2 of 2.5141(6) and 2.526(5) Å respectively are longer than that of normal Ru-Se single bond, there is a significant bonding interaction (Wiberg bond index (WBI) of 0.59) that parallels to nearly complete coupling of the Ru and Se atoms (Figure 6b, Table S1 in Supporting Information). The topological analysis[34] reveals bond critical points (BCPs) along the Se1-Ru2 and Se2-Ru2 bonds that are characterized with positive ρ and $\nabla^2(\rho)$ values indicating donor acceptor interactions (Table S5).[35] Further, the existence of BCPs has been observed for B1-B2 [ρ(0.142 a.u.) and $\nabla^2\rho$(r) (-0.244 a.u.)], and B-Se [ρ(0.109 a.u.) and $\nabla^2\rho$(r) (-0.136 a.u.)] bond paths (Figure 6a, Table S5). In addition to the bonding of the central ring, the molecular orbital analysis predicts the existence of significant bonding interaction among the Ru atoms in $[Ru_3]$ motif (HOMO-17) (Figure 6c). The σ-bonding interaction between Ru1 and Ru2 atoms by the overlap of d_z^2 orbitals can be seen in HOMO-17 (Figure 6d). The frontier orbitals HOMO and LUMO envisage the σ-bonding interaction between the boron centers and an anti-bonding interaction between the Ru2 and Ru3 atoms (Figure 6e-f), respectively.

Reactivity of *nido*-2 and *nido*-3 with $[Fe_2(CO)_9]$

Metallocenes and cyclophanes are some of the most systematically studied sandwich molecules in organometallic and organic chemistry.[36,37] The precedence of structurally characterized sandwich molecules in metallaborane and metallahetroborane chemistry are rare. Thus, in order to afford the iron analogue of **6** and **7**, we carried out the reactions of *nido*-**2** and *nido*-**3** with $[Fe_2(CO)_9]$. As shown in Scheme 4, room temperature reactions of them with $[Fe_2(CO)_9]$ resulted in the formation of *nido*-$[(Cp^*M)Fe(CO)_3B_2H_2Se_2]$, **8**-**9** (**8**: M = Co; **9**: M = Rh) and $[(Cp^*Co)Fe_3(CO)_8Se_2]$, **10** and $[(Cp^*Co)Fe_2(CO)_7Se]$, **11**. Interestingly, compound **9** is considered to be an analogue of **8**.[20]

Compound **9** is fully characterized by mass spectrometry and mutilnuclear NMR spectroscopy. The $^{11}B\{^1H\}$ NMR spectrum of

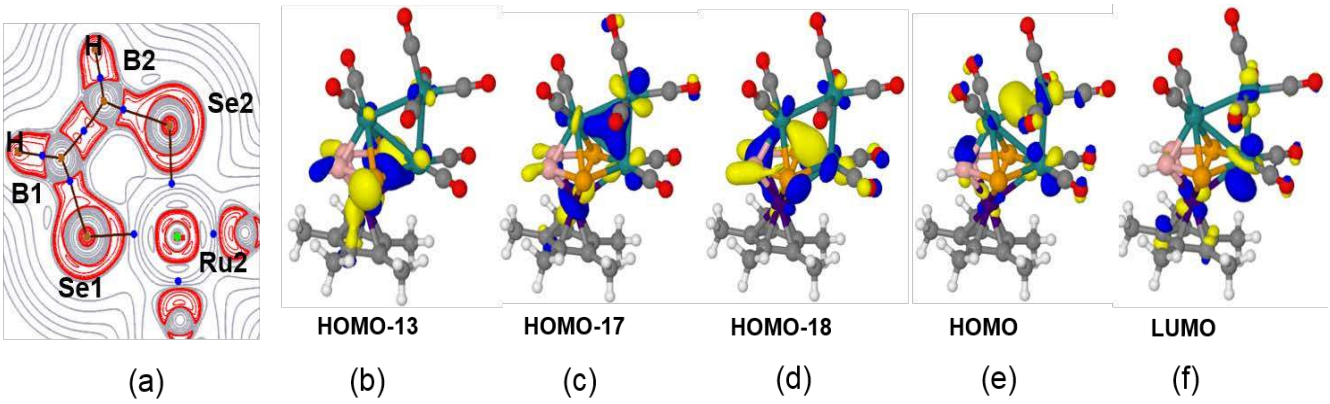

Figure 6. (a): Contour line diagrams of the Laplacian of the electron density, $\nabla^2\rho(r)$ of central ring Ru2-Se1-B1-B2-Se2 in **7** that generated using the Multiwfn program package at the PBE0/Def2-TZVP level of theory; (b-f): Illustration of molecular orbitals showing various bonding interactions. Solid red lines indicate areas of charge concentration ($-\nabla^2\rho(r) > 0$), while dashed gray lines show areas of charge depletion ($-\nabla^2\rho(r) < 0$). Solid brown lines indicate bond paths and blue dots indicate BCPs.

9 shows a sharp singlet at δ = 22.2 ppm, which is upfield shifted relative to **8** (δ = 31.2 ppm). The $^1H\{^{11}B\}$ NMR spectrum show one type of Cp* protons at δ = 1.78 ppm along with B-H_t at δ = 5.69 ppm. The mass spectrometric data (*m/z* 562.8160) suggest a molecular formula of $[(Cp^*Rh)Fe(CO)_3B_2H_2Se_2]$. The FT-IR spectrum displayed stretching frequency for CO ligands at 2054, 1997 cm^{-1} and for B-H_t at 2571 cm^{-1}. Both the experimental and the theoretical data (Tables S1 and S2) confirm the existence of plane of symmetry in **9**.

The X-ray quality crystals of **9** were obtained from hexane-layered CH_2Cl_2 solution at 3 °C. The solid-state X-ray structure of **9**, shown in Figure 7, features pentagonal bipyramidal geometry with a missing equatorial vertex. Although the Fe-B bond distance is shorter (2.199(6) Å) as compared to **8**, the B-B and B-Se bond lengths fall within the range.[19,20]

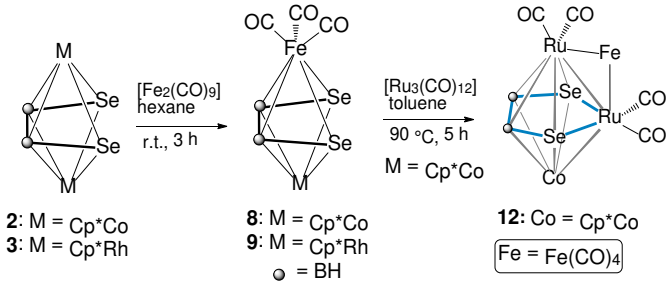

Scheme 4. Reactivity of dimetallaselenaboranes with group 8 metal carbonyl compounds.

In parallel to the formation of **8**, reaction of *nido*-**2** with $[Fe_2(CO)_9]$ yielded compounds **10** and **11**, isolated as air stable green and brown solids in low yields (Scheme S1, Supporting information). Note that reaction of *nido*-**3** with $[Fe_2(CO)_9]$ led to the formation of **9**. Compounds **10** and **11** were characterized by the ^1H, $^{13}C\{^1H\}$ NMR spectroscopy, mass spectrometry and X-ray crystallography. The ^1H NMR spectra of **10** and **11** display one type of Cp* protons. Further, presence of Cp* ligands have also been supported by $^{13}C\{^1H\}$ NMR spectra.

The solid state X-ray structure of **10**, shown in Figure S1, confirms the structural inferences made on the basis of the spectroscopic results. The molecular structure of **10** represents a new heterometallic chalcogenide cluster where the prime cluster constituents are Co, Fe and Se atoms. The asymmetric unit of **10** consist of one Co atom bonded to a Cp* ligand and three $\{Fe(CO)_2\}$ moieties which are connected through two μ-bridging CO ligands. The Co1-Fe2-Fe1-Fe3 ring bonded with two μ_4-Se atoms (Figure S1, supporting information). Overall, the core geometry of **10** can be visualized as an octahedral geometry with two bridging CO units. Compound **11** crystallizes in the monoclinic *C*2/*c* space group with the asymmetric unit consisting of one Co atom bonded to a Cp* ligand (Figure S2). The core geometry of **11** can also be well visualized as a trigonal bipyramid where the equatorial plane consists of $[CoFe_2]$ trimetallic unit.

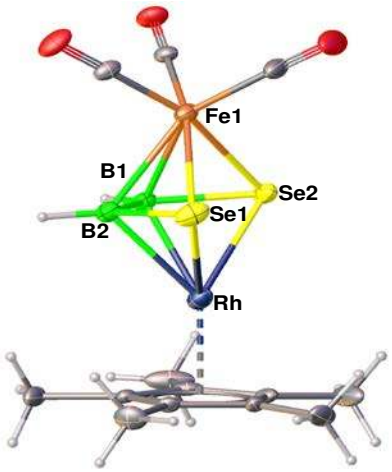

Figure 7. Molecular structure of **9**. Selected bond lengths (Å) and angles (º): Rh-B1 2.232(5), Rh-B2 2.230(5), Rh-Se1 2.4821(6), Rh-Se2 2.4792(6), Fe1-B1 2.206(5), Fe1-B2 2.199(6), Fe1-Se1 2.4535(9), B1-B2 1.699(7), B2-Se1 1.968(6), B1-Se2 1.972(5); Rh-B1-Fe1 98.8(2), Rh-B2-Fe1 99.1(2), Rh-Se1-Fe1 86.14(2), Rh-Se2-Fe1 86.28(2), B2-B1-Se2 114.9(3), B1-B2-Se1 115.6(3).

Reactivity of *nido*-8 with $[Ru_3(CO)_{12}]$

In order to close the central open ring of *nido*-**8**, we treated it with $[Ru_3(CO)_{12}]$ that indeed closed the central open ring to yield brown crystalline solid, *closo*-$[(Cp^*Co)\{\mu\text{-}\eta^5\text{:}\eta^5\text{-}B_2H_2Se_2Ru(CO)_2\}$

$Ru(CO)_2\{\mu\text{-}Fe(CO)_4\}]$, **12** in 19% yield (Scheme 4). The $^{11}B\{^1H\}$ NMR spectrum of **12** displays one resonance at δ = 23.0 ppm, similar to **6** and **7**. The IR spectrum of **12** features strong absorptions at 2054 and 1997 cm^{-1} corresponds to the terminal carbonyl groups. The mass spectrum of **12** shows molecular ion peaks (ESI^+) at *m/z* = 862.6298. In order to confirm the spectroscopic assignments and to determine the solid state structure of **12**, the X-ray diffraction analysis was undertaken. The crystal structure corresponds to a pentagonal bipyramid core consisting of Ru and Fe atoms. The molecular structure, shown in Figure 5b, is fully consistent with the solution spectroscopic data. The core geometry of **12** is similar to that of **7** with a different *exo* fragment e.g., $Fe(CO)_4$ moiety. The molecule possesses a planar $[\mu\text{-}\eta^5\text{:}\eta^5\text{-}B_2H_2Se_2Ru\{(CO)_2]$ ring (mean plane deviation 0.20 Å), sandwiched between Cp*Co unit and $[Ru(CO)_2\{\mu\text{-}Fe(CO)_4\}]$ fragment.

Conclusions

In conclusion, we have described the synthesis and chemistry of metallaheteroboranes $[(Cp^*M)_2B_2H_2E_2]$ (M = Rh and Ir: E = Se), which are analogous of $[(Cp^*Co)_2B_2H_2E_2]$ (E = S, Se). Further, we have shown the utility of these molecules to generate triple-decker sandwich dimetallaheteroboranes upon reaction with $[Ru_3(CO)_{12}]$. In addition, we have isolated and structurally characterized a novel 9-vertex *nido*-$[(Cp^*Co)_2B_5H_5Te_2]$ that represents a new metallahetroborane containing heavier chalcogen (Te) atom.

Experimental Section

General Procedures and Instrumentation: All the operations were conducted using standard Schlenk techniques under an Ar/N_2 atmosphere. Solvents were predistilled under Argon. All other reagents Cp*H, $CoCl_2$, *n*-BuLi in hexane, [$LiBH_4$·THF], S, Se, Te powders, $[Fe_2(CO)_9]$ and $[Ru_3(CO)_{12}]$ (Aldrich) were used as received. $[Cp^*Co(\mu\text{-}Cl)]_2$,[38] $[Cp^*Rh(\mu\text{-}Cl)Cl]_2$, $[Cp^*Ir(\mu\text{-}Cl)Cl]_2$,[39] *nido*-**1**,[19] *nido*-**2**,[20] *nido*-**8**,[20] and the external reference, $[Bu_4N](B_3H_8)]$,[40] for the ^{11}B NMR were synthesized by the literature methods. Thin layer chromatography was carried on 250 mm diameter aluminium supported silica gel TLC plates (MERCK TLC Plates). NMR spectra were recorded on 500 MHz Bruker FT-NMR spectrometer. Residual solvent protons were used as reference (δ, ppm, $CDCl_3$, 7.26), while a sealed tube containing $[Bu_4N(B_3H_8)]$ in C_6D_6 (^{11}B, ppm, -30.07) was used as an external reference for the ^{11}B NMR. Mass spectra were recorded in a Bruker Micro TOF-II mass spectrometer in ESI ionization mode. Infrared spectra were recorded on Jasco FT/IR-1400 spectrometer.

Synthesis of 3: In a flame-dried Schlenk tube, the brown solution of $[Cp^*Rh(\mu\text{-}Cl)Cl]_2$ (0.100 g, 0.16 mmol) in toluene (12 mL), [$LiBH_4$·THF] (0.8 mL, 1.6 mmol) was added via syringe at -78° C and allowed to warm slowly to room temperature and left stirring for one hour. Then Se powder (0.065 g, 0.81 mmol) was added to deep brown colour solution and the reaction mixture was allowed to stir at 90 °C temperature for 15 hours. The solvent was removed and the solid was extracted into hexane–CH_2Cl_2 (95:5 *v/v*) and passed through Celite. After removal of the solvent, the residue was purified on silica gel TLC plates. Elution with a hexane–CH_2Cl_2 (70:30 *v/v*) mixture yielded air stable orange compound, **3** (0.021 g, 19%) and known $[(Cp^*Rh)_2(\mu\text{-}Se)_2(\mu_3\text{-}Se)_4B_2H_2]$[5a] (0.009 g, 6%).

Reaction of $[Cp^*Rh(\mu\text{-}Cl)Cl]_2$ (0.100 g, 0.16 mmol), [$LiBH_4$·THF] (0.8 mL, 1.6 mmol) and S powder (0.025 g, 0.81 mmol) following similar reaction conditions of **3** yielded known $[(Cp^*Rh)_2B_3H_7]$[25] and $[(Cp^*Rh)_2(\mu\text{-}S)_2(\mu_3\text{-}S)_4B_2H_2]$.[5a]

3. HRMS (ESI^+): *m/z* calculated for $C_{20}H_{32}B_2Rh_2Se_2Na$ 682.9028 $[M + Na]^+$ found: 682.8986;$^{11}B\{^1H\}$ NMR (160 MHz, $CDCl_3$, 22 °C): δ = 23.9 (s, 2B); $^1H\{^{11}B\}$ NMR (500 MHz, $CDCl_3$, 22 °C): δ = 1.77 (s, 30H, Cp*), 4.50 (s, 2B-H_t); $^{13}C\{^1H\}$ NMR (125 MHz, $CDCl_3$, 22 °C): δ = 95.6 (s C_5Me_5), 10.0 (s C_5Me_5); IR (DCM, cm^{-1}): $\tilde{\nu}$ = 2560 (BH_t).

Synthesis of 4: In a flame-dried Schlenk tube, the yellow solution of $[Cp^*Ir(\mu\text{-}Cl)Cl]_2$ (0.100 g, 0.12 mmol) in toluene (12 mL), [$LiBH_4$·THF] (0.6 mL, 1.25 mmol) was added via syringe at -78° C and allowed to warm slowly to room temperature and left stirring for one hour. Then Se powder (0.050 g, 0.62 mmol) was added to colourless colour solution and the reaction mixture was allowed to stir at 70 °C temperature for 18 hours. The solvent was removed and the solid was extracted into hexane–CH_2Cl_2 (95:5 *v/v*) and passed through Celite. After removal of the solvent, the residue was purified on silica gel TLC plates. Elution with a hexane–CH_2Cl_2 (70:30 *v/v*) mixture yielded air stable yellow compound, **4** (0.011 g, 10%).

Under similar reaction conditions, $[Cp^*Ir(\mu\text{-}Cl)Cl]_2$ (0.100 g, 0.12 mmol), [$LiBH_4$·THF] (0.6 mL, 1.25 mmol) and S powder (0.020 g, 0.62 mmol) yielded Cp^*IrH_4 as major product.[26]

4. HRMS (ESI^+): *m/z* calculated for $C_{20}H_{33}B_2Ir_2Se_2$ 841.0358 $[M + H]^+$; found: 841.0363; $^{11}B\{^1H\}$ NMR (160 MHz, $CDCl_3$, 22 °C): δ = 7.3 (s, 2B); $^1H\{^{11}B\}$ NMR (500 MHz, $CDCl_3$, 22 °C): 1.84 (s, 30H, Cp*), 2.98 (s, 2B-H_t); $^{13}C\{^1H\}$ NMR (125 MHz, $CDCl_3$, 22 °C): δ = 90.3 (s, C_5Me_5), 9.8, (s, C_5Me_5); IR (DCM, cm^{-1}): $\tilde{\nu}$ = 2571 (BH_t).

Synthesis of 5: In a pre-dried Schlenk tube a brown $[Cp^*Co(\mu\text{-}Cl)]_2$ (0.100 g, 0.218 mmol) was dissolved in dry toluene (10 mL). To that solution, [$LiBH_4$·THF] (1.1 mL, 2.2 mmol) was added via a syringe at -78 °C and allowed to stay for half an hour and slowly warmed to room temperature. Then, Te powder (0.142 g, 1.1 mmol) was added to the red brown solution and the mixture was heated at 90 °C for 18 hours. The solvent was evacuated and the residue was extracted into hexane–CH_2Cl_2 (80:20 *v/v*) and passed through Celite. After removal of the solvent the resulting solid was separated by TLC on silica gel TLC plates. Elution with hexane–CH_2Cl_2 (60:40 *v/v*) yielded violet compound $[(Cp^*Co)_2B_5H_5Te_2]$, **5** (0.025 g, 16%), brown $[(Cp^*Co)_2B_4H_6]$, (0.015 g, 16%) and yellow $[(Cp^*Co)_3B_4H_4]$, (0.016 g, 12%).

Note that, the compounds $[(Cp^*Co)_2B_4H_6]$ and $[(Cp^*Co)_3B_4H_4]$ have been synthesized and characterized in comparison with the spectroscopic data reported earlier by Grimes *et al.* by the reaction of Cp*Li, $CoCl_2$ with $[B_5H_8]^-$.[24]

5. HRMS (ESI^+): *m/z* calculated for $C_{20}H_{35}B_5Co_2Te_2Na$ 730.9890, $[M + Na]^+$ found: 730.9910; $^{11}B\{^1H\}$ NMR (160 MHz, $CDCl_3$, 22 °C): δ = -3.6 (s, 4B), -8.5 ppm (s, 1B); $^1H\{^{11}B\}$ NMR (500 MHz, $CDCl_3$, 22 °C): δ = 1.79 (s, 30H, Cp*), 2.97 (s, 4B-H_t), 6.00 ppm (s, 1B-H_t); $^{13}C\{^1H\}$ NMR (125 MHz, $CDCl_3$, 22 °C): δ = 92.5 (s, C_5Me_5), 10.9 ppm (s, C_5Me_5); IR (DCM, cm^{-1}): $\tilde{\nu}$ = 2497 (BH_t).

Synthesis of 6 and 7: In a flame-dried Schlenk tube, *nido*-$[(Cp^*Co)_2B_2H_2S_2]$, **1** (0.060 g, 0.126 mmol) was dissolved in toluene (6

mL) and $[Ru_3(CO)_{12}]$ (0.081 g, 0.126 mmol) was added to that solution. The reaction mixture was allowed to stir at 90 °C temperature for 7 hours. The solvent was removed and the solid was extracted into hexane–CH_2Cl_2 (95:5 *v/v*) and passed through Celite. After removal of the solvent, the residue was purified on silica gel TLC plates. Elution with a hexane–CH_2Cl_2 (70:30 *v/v*) mixture yielded air stable brown compound, **6** (0.028 g, 27%).

In a similar reaction conditions, the reaction of *nido*-**2** (0.060 g, 0.105 mmol) with $[Ru_3(CO)_{12}]$ (0.067 g, 0.105 mmol) led to the isolation of the green, **7** (0.031 g, 32%). Similar reaction work up and purification methods were employed for compound **7** as employed for the compound **6**.

6. HRMS (ESI$^+$): *m/z* calculated for $C_{18}H_{18}B_2CoRu_3O_8S_2$ 812.7092 [M + H]$^+$, found: 812.7104; $^{11}B\{^1H\}$ NMR (160 MHz, $CDCl_3$, 22 °C): δ = 19.9 (s, 2B); $^1H\{^{11}B\}$ NMR (500 MHz, $CDCl_3$, 22 °C): δ = 1.71 (s, 15H, Cp*), 4.98 (s, 2B-H_t); $^{13}C\{^1H\}$ NMR (125 MHz, $CDCl_3$, 22 °C): δ = 197.4, 186.1 (*C*O), 95.0 (s C_5Me_5), 11.2 (s, C_5Me_5); IR (DCM, cm^{-1}): $\tilde{\nu}$ = 2523 (BH_t), 1997, 1934 (terminal C-O stretching).

7. HRMS (ESI$^+$): *m/z* calculated for $C_{18}H_{17}B_2CoRu_3O_8Se_2Na$ 930.5800 [M + Na]$^+$, found 930.5797; $^{11}B\{^1H\}$ NMR (160 MHz, $CDCl_3$, 22 °C): δ = 22.3 (s, 2B); $^1H\{^{11}B\}$ NMR (500 MHz, $CDCl_3$, 22 °C): δ = 1.66 (s, 15H, Cp*), 6.05 (s, 2B-H_t); $^{13}C\{^1H\}$ NMR (125 MHz, $CDCl_3$, 22 °C,): δ = 197.1 (*C*O), 93.7 (s, C_5Me_5), 11.3 (s, C_5Me_5); IR (DCM, cm^{-1}): $\tilde{\nu}$ = 2539 (BH_t), 2080, 2002, 1924 (terminal CO stretching).

Synthesis of 9. In a flame-dried Schlenk tube, *nido*-$[(Cp^*Rh)_2B_2H_2Se_2]$, **3** (0.060 g, 0.091 mmol) and $[Fe_2(CO)_9]$ (0.066 g, 0.181 mmol) were dissolved in hexane (10 mL) and allowed to stir at room temperature for **3** hours. The solvent was removed under vacuum and the solid was extracted into hexane-CH_2Cl_2 (90:10 *v/v*) and passed through Celite. After the removal of solvent the resultant residue was chromatographed on silica gel TLC plates. Elution with a hexane–CH_2Cl_2 (80:20 *v/v*) mixture yielded air stable orange $[(Cp^*Rh)Fe(CO)_3B_2H_2Se_2]$, **9** (0.011 g, 21%).

9. HRMS (ESI$^+$): *m/z* calculated for $C_{13}H_{18}B_2RhFeO_3Se_2$ 562.8176 [M + H]$^+$, found 562.8160; $^{11}B\{^1H\}$ NMR (160 MHz, $CDCl_3$, 22 °C): δ = 22.2 (s, 2B); $^1H\{^{11}B\}$ NMR (500 MHz, $CDCl_3$, 22 °C): δ = 1.78 (s, 15H, Cp*), 5.69 (s, 2B-H_t); IR (DCM, cm^{-1}): $\tilde{\nu}$ = 2571 (BH_t), 2054, 1997 (terminal CO stretching).

Synthesis of 10 and 11: In a flame-dried Schlenk tube, *nido*-$[(Cp^*Co)_2B_2H_2Se_2]$ **2** (0.10 g, 0.174 mmol) was dissolved in hexane (6 mL) and then it was allowed to react with $[Fe_2(CO)_9]$ (0.13 g, 0.349 mmol) at room temperature for 3 hours. The solvent was removed under vacuum and the solid was extracted into hexane-CH_2Cl_2 (90:10 *v/v*) and passed through Celite. After the removal of solvent the resultant residue was chromatographed on silica gel TLC plates. Elution with a hexane–CH_2Cl_2 (80:20 *v/v*) mixture yielded air stable green $[(Cp^*Co)Fe_3(CO)_8Se_2]$, **10** (0.018 g, 14%), brown $[(Cp^*Co)Fe_2(CO)_7Se]$, **11** (0.021 g, 20%) and known violet **8** $[(Cp^*Co)Fe(CO)_3B_2H_2Se_2]$ (0.28 g, 31%).

10. HRMS (ESI$^+$): *m/z* calculated for $C_{18}H_{16}CoFe_3O_8Se_2$ 746.6555 [M + H]$^+$ found: 746.6562; ^1H NMR (500 MHz, $CDCl_3$, 22 °C): δ = 1.82 (s, 15H, Cp*); $^{13}C\{^1H\}$ NMR (125 MHz, $CDCl_3$, 22 °C): δ = 210.9 (s, *C*O), 98.1 (s, C_5Me_5), 10.4 (s, C_5Me_5); IR (DCM, cm^{-1}): $\tilde{\nu}$ = 2060, 1986 (terminal CO stretching).

11. MS (ESI$^+$): *m/z* calculated for $C_{17}H_{16}CoFe_2O_7Se$ 582.8091 [M + H]$^+$ found: 582.8085; ^1H NMR (500 MHz, $CDCl_3$, 22 °C): δ = 2.24 (s, 15H, Cp*); $^{13}C\{^1H\}$ NMR (125 MHz, $CDCl_3$, 22 °C): δ = 206.7 (s, *C*O), 97.1 (s, C_5Me_5), 12.8 (s, C_5Me_5); IR (DCM, cm^{-1}): $\tilde{\nu}$ = 2038, 1991, 1960 (terminal CO stretching).

Synthesis of 12: In a flame-dried Schlenk tube, *nido*-$[(Cp^*Co)Fe(CO)_3B_2H_2Se_2]$, **8** (0.060 g, 0.116 mmol) was stirred in toluene (6 mL) with $[Ru_3(CO)_{12}]$ (0.074 g, 0.116 mmol) at 90 °C temperature for 5 hours. The solvent was removed under vacuum and the residual solid was extracted into hexane-CH_2Cl_2 (95:5, *v/v*) and passed through Celite. After removal of the solvent, the residue was chromatographed on silica gel TLC plates. Elution with a hexane-CH_2Cl_2 (70:30, *v/v*) mixture yielded air stable brown $[(Cp^*Co)FeRu_2(CO)_8B_2H_2Se_2]$, **12** (0.019g, 19%) and green $[(Cp^*Co)Ru_3(CO)_8B_2H_2Se_2]$, **7** (0.016 g, 14%).

12. HRMS (ESI$^+$): *m/z* calculated for $C_{18}H_{18}B_2FeRu_2CoSe_2$ 862.6287 [M + H]$^+$; found 862.6298; $^{11}B\{^1H\}$ NMR (160 MHz, $CDCl_3$, 22 °C): δ = 23.0 (s, 2B); $^1H\{^{11}B\}$ NMR (500 MHz, $CDCl_3$, 22 °C): δ = 1.65 (s, 15H, Cp*), 6.05 (s, 2B-H_t); $^{13}C\{^1H\}$ NMR (125 MHz, $CDCl_3$, 22 °C): δ = 196.2 (*C*O), 94.1 (s, C_5Me_5), 11.3 (s, C_5Me_5); IR (DCM, cm^{-1}): $\tilde{\nu}$ = 2461 (BH_t), 2054, 1997 (terminal C-O stretching).

X-ray crystal structure determinations. Crystal diffraction data of **3** and **7** were collected and integrated using a D8 VENTURE Bruker AXS diffractometer, with multilayer monochromated $Mo_{K\alpha}$ (λ = 0.71073 Å) radiation. The crystal data for **4**, **5**, **9**-**11** and **12**, were collected on a Bruker APEXII AXS diffractometer, equipped with a CCD detector, using $Mo_{K\alpha}$ radiation (λ = 0.71073 Å). The structures were solved by direct methods using the SIR97[41] program and then refined with full-matrix least-squares methods based on F^2 (SHELXL-2014)[42] with the aid of the WINGX program. All non-hydrogen atoms were refined with anisotropic atomic displacement parameters, except boron-linked hydrogen atoms that were introduced in the structural model through Fourier difference map analysis. Hydrogen atoms were finally included in their calculated positions.

Crystal data for 3: CCDC 1586318, $C_{20}H_{32}B_2Rh_2Se_2$, M_r = 657.81, monoclinic, *P21/c*, a = 11.0070(13) Å, b = 16.043(2) Å, c = 14.1958(18) Å, β = 112.055(4)°, V = 2323.3(5) Å^3, Z = 4, ρ_{calcd} = 1.881 mg/m^3, μ = 4.556 mm^{-1}, F(000) = 1280, R_1 = 0.0218, wR_2 = 0.0493, 5302 independent reflections [2θ ≤ 50.48°] and 251 parameters, Goodness-of-fit on F^2 = 1.087.

Crystal data for 4: CCDC 1586319, $C_{20}H_{32}B_2Ir_2Se_2$, M_r = 836.39, monoclinic, *C2/c*, a = 20.4852(5) Å, b = 15.1280(4) Å, c = 16.3205(3) Å, β = 108.2660(11)°, V = 4802.9(2) Å^3, Z = 8, ρ_{calcd} = 2.313 mg/m^3, μ = 14.105 mm^{-1}, F(000) = 3072, R_1 = 0.0261, wR_2 = 0.0526, 4234 independent reflections [2θ ≤ 49.994°] and 245 parameters, Goodness-of-fit on F^2 = 0.987.

Crystal data for 5: CCDC 1560400, $C_{20}H_{35}B_5Co_2Te_2$, M_r = 702.59, monoclinic, *C2/c*, a = 15.4187(12) Å, b = 8.1411(5) Å, c = 20.938(2) Å, β = 107.167(4), V = 2511.2(3) Å^3, Z = 4, ρ_{calcd} = 1.858 mg/m^3, μ = 3.604 mm^{-1}, F(000) = 1352, R_1 = 0.0249, wR_2 = 0.0585, 2216 independent reflections [2θ ≤ 49.99°] and 132 parameters, Goodness-of-fit on F^2 = 1.060.

Crystal data for 7: CCDC 1560396, $C_{18}H_{17}B_2CoO_8Ru_3Se_2$, M_r = 902.99, orthorhombic, $P2_12_12_1$, a = 10.8925(10) Å, b = 14.0241(13) Å, c = 16.8780(13) Å, V = 2578.2(4) Å^3, Z = 4, ρ_{calcd} = 2.326 mg/m^3, μ = 5.219 mm^{-1}, F(000) = 1704, R_1 = 0.0195, wR_2 = 0.0420, 5834 independent reflections [2θ ≤ 54.96°] and 319 parameters, Goodness-of-fit on F^2 = 1.079.

Crystal data for 9: CCDC 1589292, $C_{13}H_{17}B_2FeO_3RhSe_2$, M_r = 559.56, triclinic, *P-1*, a = 8.3383(4) Å, b = 9.8899(5) Å, c = 11.9936(6) Å, α = 81.201(2), β = 85.229(2)°, γ = 70.571(2)°, V = 921.20(8) Å^3, Z = 2, ρ_{calcd} = 2.017 mg/m^3, μ = 5.638 mm^{-1}, F(000) = 536, R_1 = 0.0293, wR_2 = 0.0561, 3227 independent reflections [2θ ≤ 49.994°], 200 parameters and Goodness-of-fit on F^2 = 1.040.

Crystal data for 10: CCDC 1560397, $C_{18}H_{15}CoFe_3O_8Se_2$, M_r = 743.70, monoclinic, *Cc*, a = 17.1818(8) Å, b = 10.4178(5) Å, c = 14.2140(6) Å, β = 111.053(2)°, V = 2374.42(19) Å^3, Z = 4, ρ_{calcd} = 2.080 mg/m^3, μ = 5.589 mm^{-1}, F(000) = 1440, R_1 = 0.0311, wR_2 = 0.0750, 3850 independent reflections [2θ ≤ 49.99°] and 276 parameters, Goodness-of-fit on F^2 = 1.037.

Crystal data for 11: CCDC 1560398, $C_{17}H_{15}CoFe_2O_7Se$, M_r = 580.88, monoclinic, *C2/c*, a = 19.2335(7) Å, b = 8.5091(3) Å, c = 27.0380(9) Å, β = 114.023(2)°, V = 4041.7(3) Å^3, Z = 8, ρ_{calcd} = 1.909 mg/m^3, μ = 4.064 mm^{-1}, F(000) = 2288, R_1 = 0.0407, wR_2 = 0.0648, 4606 independent reflections [2θ ≤ 54.97°] and 258 parameters, Goodness-of-fit on F^2 = 1.029.

Crystal data for 12: CCDC 1560399, $C_{18}H_{17}B_2CoFeO_8Ru_2Se_2$, M_r = 857.77, monoclinic, $P2_1/n$, a = 8.7864(2) Å, b = 17.5214(4) Å, c = 17.3426(4) Å, β = 99.5134(10)°, V = 2633.17(10) Å^3, Z = 4, ρ_{calcd} = 2.164 mg/m^3, μ = 5.088 mm^{-1}, F(000) = 1632, R_1 = 0.0309, wR_2 = 0.0654, 4639 independent reflections [2θ ≤ 50.00°] and 320 parameters, Goodness-of-fit on F^2 = 1.018.

Computational Details. Quantum chemical calculations using DFT methods were carried out on compounds **2**-**4**, **5'** and **7**-**9** (Cp analogue) as employed in the Gaussin09 package.[43] All the geometry optimizations were carried out in gaseous state without any symmetry constraints, (no solvent effect) using PBE0 functional[44] in combination with triple-ζ quality basis set Def2-TZVP. Computation of the NMR shielding tensors employed gauge-including atomic orbitals (GIAOs),[45] using the implementation of Schreckenbach, Wolff, Ziegler, and co-workers.[46] The projected ^{11}B chemical shift values, determined at the PBE0/Def2-TZVP level of calculations, were referenced to B_2H_6 (PBE0/Def2-TZVP, B shielding constant 80.03 ppm), and these chemical shift values (δ) were then converted to the standard $BF_3{\cdot}OEt_2$ scale using the experimental value of +16.6 ppm for B_2H_6. ^{1}H chemical shifts were referenced to TMS ($SiMe_4$). Natural bond orbital (NBO) analysis[47] within the Gaussian09 package was carried out at the same level of theory. Wiberg bond indexes (WBI)[48] values on some selected bonds were obtained on natural bond orbital (NBO) analysis. The Jmol package[49] was used for the visualizations. The two dimensions electron density and Laplacian electronic distribution plots were generated using Multiwfn package.[50]

Acknowledgements

This project was supported Council of Scientific and Industrial Research (CSIR; No. 01(2837)/15/EMR-II), New Delhi, India B.J. and R.R. thank University Grants Commission, India for fellowships. S.K.B. thanks IIT Madras for research fellowship. We thank V. Ramkumar, P. K. Sudhadevi Antharjanam (SAIF, IIT Madras) for X-ray analysis and Professor Jean-François Halet, University of Rennes 1, France for helpful discussions. IIT Madras is gratefully acknowledged for computational facilities.

Keywords: Group 9 • heteroboranes • chalcogens • triple decker • metal carbonyls

[1] S. Luaces, J. Bould, R. Macías, R. Sancho, F. J. Lahoza, L. A. Oro, *Dalton Trans.* **2012**, *41*, 11627-11634.

[2] a) L. Barton, D. K. Srivastava (chapter 8), in *Comprehensive Organometallic Chemistry II*, *Vol* 1 (Eds.: E. Abel, F. G. A. Stone, G. Wilkinson.), Pergamon, New York, **1995**, pp. 275-373; b) T. P. Fehlner, J.-F. Halet, J.-Y. Saillard, *Molecular Clusters. A Bridge to Solid State Chemistry*. Cambridge, **2008**, pp 8774-8775.

[3] a) R. Macias, J. Holub, J. D. Kennedy, B. Stibr, M. Thornton-Pett, *J. Chem. Soc., Chem. Commun.* **1994**, 2265-2266; b) K. Mazighi, P. J. Carroll, L. G. Sneddon, *Inorg. Chem.* **1992**, *31,* 3197-3204; c) M. Bown, X. L. R. Fontaine, N. N. Greenwood, J. D. Kennedy, *Z. Anorg. Allg. Chem.* **1991**, *602*, 17-29; d) G. Ferguson, M. C. Jennings, A. J. Lough, S. Coughlan, T. R. Spalding, J. D. Kennedy, X. L. R. Fontaine, B. Stibr, *J. Chem. Soc. Chem. Commun.* **1990**, 891-894.

[4] a) Y.-H. Kim, R. Greatrex, J. D. Kennedy, *Collect. Czech. Chem. Commun.* **1997**, *62*, 1289-1298; b) J. Bould, N. P. Rath, L. Barton, *Organometallics* **1996**, *15*, 4916-4929.

[5] a) S. K. Barik, C. E. Rao, K. Yuvaraj, R. Jagan, S. Kahlal, J.-F. Halet, S. Ghosh, *Eur. J. Inorg. Chem.* **2015**, 5556-5562; b) C. E. Rao, K. Yuvaraj, S. Ghosh, *J. Organomet. Chem.* **2015**, *776*, 123-128; c) R. S. Dhayal, V. Ramkumar, S. Ghosh, *Polyhedron* **2011**, *30*, 2062-2066; d) R. S. Dhayal, K. K. V. Chakrahari, B. Varghese, S. M. Mobin, S. Ghosh, *Inorg. Chem.* **2010**, *49*, 7741-7747; e) S. Sahoo, S. M. Mobin, S. Ghosh, *J. Organomet. Chem.* **2010**, *695*, 945-949; f) K. K. Chakrahari, D. Sharmila, S. K. Barik, B. Mondal, B. Varghese, S. Ghosh, *J. Organomet. Chem.* **2014**, *749*, 188-196.

[6] S. L. Shea, T. D. McGrath, T. Jelínek, B. Štíbr, M. Thornton-Pett, J. D. Kennedy, *Inorg. Chem. Commun.* **1998**, *1*, 97-100.

[7] A. C. Mateo, B. Calvo, R. Macías, M. J. Artigas, F. J. Lahoz, L. A. Oro, *Dalton Trans.* **2015**, *44*, 9004-9013.

[8] a) Á. Álvarez, R. Macías, J. Bould, C. Cunchillos, F. J. Lahoz, L. A. Oro, *Chem. Eur. J.* **2009**, *15*, 5428-5431; b) Á. Álvarez, R. Macías, M. J. Fabra, F. J. Lahoz, L. A. Oro, *J. Am. Chem. Soc.* **2008**, *130*, 2148-2149; c) Á. Álvarez, R. Macías, J. Bould, M. J. Fabra, F. J. Lahoz, L. A. Oro, *J. Am. Chem. Soc.* **2008**, *130*, 11455-11466.

[9] a) S. K. Bose, S. M. Mobin, S. Ghosh, *J. Organomet. Chem.* **2011**, *696*, 3121-3126; b) A. Hammerschmidt, M. Döch, S. Pütz, B. Krebs, *Z. Anorg. Allg. Chem.* **2005**, *631*, 1125-1128; c) N. C. Norman, A. G. Orpen, M. J. Quayle, C. R. Rice, *New J. Chem.* **2000**, *24*, 837-839; d) Faridoon, O. N. Dhubhghaill, T. R. Spalding, G. Ferguson, B. Kaitner, X. L. R. Fontaine, J. D. Kennedy, *J. Chem. Soc., Dalton Trans.* **1989**, 1657-1668; e) G. D. Friesen, A. Barriola, P. Daluga, P. Ragatz, J. C. Huffman, L. J. Todd, *Inorg. Chem.* **1980**, *19*, 458-462.

[10] a) G. Ferguson, J. F. Gallagher, J. D. Kennedy, A.-M. Kelleher, T. R. Spalding, *Dalton Trans.* **2006**, 2133-2139; b) D. O'Connell, J. C. Patterson, T. R. Spalding, G. Ferguson, J. F. Gallagher, Y. Li, J. D. Kennedy, R. Macías, M. Thornton-Pett, J. Holub, *J. Chem. Soc., Dalton Trans.* **1996**, 3323-3333; c) G. Ferguson, J. F. Gallagher, M. N. McGrath, J. P. Sheehan, T. R. Spalding, J. D. Kennedy, *J. Chem. Soc., Dalton Trans.* **1993**, 27-34; d) G. Ferguson, A. J. Lough, Faridoon, O. N. Dhubhghaill, M. N. McGrath, T. R. Spalding, J. D. Kennedy, X. L. R. Fontaine, *J. Chem. Soc., Dalton Trans.* **1990**, 1831-1839; e) Faridoon, M. McGrath, T. R. Spalding, X. L. R. Fontaine, J. D. Kennedy, M. Thornton-Pett, *J. Chem. Soc., Dalton Trans.* **1990**, 1819-1829.

[11] a) K. K. V. Chakrahari, R. Ramalakshmi, D. Sharmila, S. Ghosh, *J. Chem. Sci.* **2014**, *126*, 1597-1603; b) D. K. Roy, S. K. Bose, K. Geetharani, K. K. V. Chakrahari, S. M. Mobin, S. Ghosh, *Chem. Eur. J.* **2012**, *18*, 9983-9991; c) A. Thakur, S. Sao, V. Ramkumar, S. Ghosh, *Inorg. Chem.* **2012**, 51, 8322-8330.

[12] a) K. K. V. Chakrahari, A. Thakur, B. Mondal, V. Ramkumar, S. Ghosh, *Inorg. Chem.* **2013**, *52*, 7923-7932; b) S. J. Ponniah, J. K. Bharathan, S.

K. Bose, S. Ghosh, *J. Organomet. Chem.* **2012**, *721*, 42-48; c) D. A. Lesch, T. B. Rauchfuss, *Organometallics* **1982**, *1*, 499-506.

[13] a) M. G. Chowdhury, S. K. Barik, K. Saha, B. Kirubakaran, A. Banerjee, V. Ramkumar, S. Ghosh, *Inorg. Chem.* **2018**, *57*, 985-994; b) P. Shankhari, D. K. Roy, K. Geetharani, R. S. Anju, B. Varghese, S. Ghosh, *J. Organomet. Chem.* **2013**, *747*, 249-253; c) S. K. Bose, S. M. Mobin, S. Ghosh, *J. Organomet. Chem.* **2011**, *696*, 3121-3126; d) S. K. Bose, K. Geetharani, V. Ramkumar, B. Varghese, S. Ghosh, *Inorg. Chem.* **2010**, *49*, 2881-2888.

[14] a) B. S. Krishnamoorthy, A. Thakur, K. K. V. Chakrahari, S. K. Bose, P. Hamon, T. Roisnel, S. Kahlal, S. Ghosh, J.-F. Halet, *Inorg. Chem.* **2012**, *51*, 10375-10383; b) K. Geetharani, S. K. Bose, S. Ghosh, *Pure Appl. Chem.* **2012**, *84*, 2233-2241; c) K. Geetharani, S. K. Bose, S. Sahoo, S. Ghosh, *Angew. Chem.* **2011**, *123*, 3994-3997; *Angew. Chem., Int. Ed.* **2011**, *50*, 3908-3911; d) A. Thakur, K. K. V. Chakrahari, B. Mondal, S. Ghosh, *Inorg. Chem.* **2013**, *52*, 2262-2264.

[15] K. Geetharani, S. K. Bose, D. Basak, V. M. Suresh, S. Ghosh, *Inorg. Chim. Acta* **2011**, *372*, 42-46.

[16] B. Mondal, M. Bhattacharyya, B. Varghese, S. Ghosh, *Dalton Trans.* **2016**, *45*, 10999-11007.

[17] a) R. N. Grimes, *Acc. Chem. Res.* **1978**, *11*, 420-427; b) R. N. Grimes, *Coord. Chem. Rev.* **1979**, *28*, 47-96.

[18] R. P. Micciche, P. J. Carroll, L. G. Sneddon, *Organometallics* **1985**, *4*, 1619-1623.

[19] D. Sharmila, R. Ramalakshmi, K. K. V. Chakrahari, B. Varghese, S. Ghosh, *Dalton Trans.* **2014**, *43*, 9976-9985.

[20] S. K. Barik, V. Dorcet, T. Rosinel, J.-F. Halet, S. Ghosh, *Dalton Trans.* **2015**, *44*, 14403-14410.

[21] Note that, similar reactions have been carried out in presence of S powder, which led to the formation of known compounds as well as other unknown compounds with poor yields, which we couldn't isolate.

[22] a) D. M. P. Mingos, *Nat. Phys. Sci.* **1972**, *236*, 99-102; b) D. M. P. Mingos, *Acc. Chem. Res.* **1984**, *17*, 311-319.

[23] a) A. K. Sharma, H. Joshi, R. Bhaskar, A. K. Singh, *Dalton Trans.* **2017**, *46*, 2228-2237; b) S. K. Barik, M. G. Chowdhury, S. De, P. Parameswaran, S. Ghosh, *Eur. J. Inorg. Chem.* **2016**, 4546-4550; c) R. Borthakur, B. Mondal, P. Nandi, S. Ghosh, *Chem. Commun.* **2016**, *52*, 3199-3202; d) D. K. Roy, B. Mondal, P. Shankhari, R. S. Anju, K. Geetharani, S. M. Mobin, S. Ghosh, *Inorg. Chem.* **2013**, *52*, 6705-6712.

[24] a) T. L. Venable, R. N. Grimes, *Inorg. Chem.* **1982**, *21*, 887-895; b) Y. Nishihara, K. J. Deck, M. Shang, T. P. Fehlner, B. S. Haggerty, A. L. Rheingold, *Organometallics* **1994**, *13,* 4510-4522.

[25] X. Lei, M. Shang, T. P. Fehlner, *J. Am. Chem. Soc.* **1999**, *121*, 1275-1287.

[26] X. Lei, A. K. Bandyopadhyay, M. Shang, T. P. Fehlner, *Organometallics* **1999**, *18*, 2294-2296.

[27] A. Ceriotti, G. Longoni, M. Manassero, M. Perego, M. Sansoni, *Inorg. Chem.* **1985**, *24*, 117-120.

[28] M. L. Steigerwald, T. Siegrist, S. M. Stuczynski, *Inorg. Chem.* **1991**, *30*, 4940-4945.

[29] a) S. Ghosh, M. Shang, T. P. Fehlner, *J. Organomet. Chem.* **2000**, *92*, 614-615; b) S. Ghosh, X. Lei, M. Shang, T. P. Fehlner, *Inorg. Chem.* **2000**, *39*, 5373-5382.

[30] S. Ghosh, A. M. Beatty, T. P. Fehlner, *J. Am. Chem. Soc.* **2001**, *123*, 9188-9189.

[31] S. Ghosh, M. Shang, T. P. Fehlner, *J. Am. Chem. Soc.* **1999**, *121*, 7451-7452.

[32] J. Bould, N. P. Rath, L. Barton, *Angew. Chem.* **1995**, *107*, 1744-1746; *Angew. Chem., Int. Ed.* **1995**, *34*, 1641-1643.

[33] E. D. Jemmis, M. N. Balakrishnarajan, P. D. Pancharatna, *Chem. Rev.* **2002**, *102*, 93-144.

[34] The topological parameters calculated for the Ru2-Se1, Ru2-Se2, B1-B2, B1-Se1 and B2-Se2 bond paths in Ru2-Se1-B1-B2-Se2 plane i.e., the electron density ρ at the bond critical points (BCPs (3,-1)), the Laplacian of the density $\nabla^2\rho$ are listed in Table S5.

[35] U. Flierler, M. Burzler, D. Leusser, J. Henn, H. Ott, H. Braunschweig, D. Stalke, *Angew. Chem.* **2008**, *120*, 4393-4397; *Angew. Chem. Int. Ed.* **2008**, *47*, 4321-4325.

[36] a) R. A. Musgrave, A. D. Russell, I. Manners, *Organometallics* **2013**, *32*, 5654-5667; b) H. Braunschweig, T. Kupfer, *Acc. Chem. Res.* **2010**, *43*, 455-465; c) X.-K. Huo, G. Su, G.-X. Jin, *Dalton Trans.* **2010**, *39*, 1954-1961.

[37] a) A. D. Russell, R. A. Musgrave, L. K. Stoll, P. Choi, H. Qiu, I. Manners, *J. Organomet. Chem.* **2015**, 784, 24-30; b) Y.-F. Han, Y. Fei, G.-X. Jin, *Dalton Trans.* **2010**, *39*, 3976-3984; c) Y.-F. Han, W.-G. Jia, W.-B. Yu, G.-X. Jin, *Chem. Soc. Rev.* **2009**, *38*, 3419-3434.

[38] a) U. Kolle, F. Khouzami, B. Fuss, *Angew. Chem.* **1982**, *94*, 132-133; *Angew. Chem. Int. Ed.* **1982**, *21*, 131-132; b) T. Yoshino, H. Ikemoto, S. Matsunaga, M. Kanai, *Angew. Chem.* **2013**, *125*, 2263-2267; *Angew. Chem. Int. Ed.* **2013**, *52*, 2207-2211.

[39] a) C. White, A. Yates, P. M. Maitlis, *Inorg. Synth.* **1992**, *29*, 228-234; b) J. W. Kang, K. Moseley, P. M. Maitlis, *J. Am. Chem. Soc.* **1969**, *91*, 5970-5977.

[40] G. E. Ryschkewitsch, K. C. Nainan, *Inorg. Synth.* **1974**, *15*, 111-118.

[41] SIR92, A. Altornare, G. Cascarano, C. Giacovazzo, A. Guagliardi, *J. Appl. Cryst.* **1993**, *26*, 343-350.

[42] a) G. M. Sheldrick, *SHELXS-97*; University of Gottingen: Germany, **1997**; b) G. M. Sheldrick, *SHELXL, Program for Crystal Structure Refinement*, version 2014/3, University of Göttingen, Germany, **2014**.

[43] M. J. Frisch, G. W. Trucks, H. B. Schlegel, G. E. Scuseria, M. A. Robb, J. R. Cheeseman, G. Scalmani, V. Barone, B. Mennucci, G. A. Petersson, H. Nakatsuji, M. Li, X. Caricato, H. P. Hratchian, A. F. Izmaylov, J. Bloino, G. Zheng, J. L. Sonnenberg, M. Hada, M. Ehara, K. Toyota, R. Fukuda, J. Hasegawa, M. Ishida, T. Nakajima, Y. Honda, O. Kitao, H. Nakai, T. Vreven, J. A., Jr. Montgomery, J. E. Peralta, F. Ogliaro, M. Bearpark, J. J. Heyd, E. Brothers, K. N. Kudin, V. N. Staroverov, T. Keith, R. Kobayashi, J. Normand, K. Raghavachari, A. Rendell, J. C. Burant, S. S. Iyengar, J. Tomasi, M. Cossi, N. Rega, J. M Millam, M. Klene, J. E. Knox, J. B. Cross, V. Bakken, C. Adamo, J. Jaramillo, R. Gomperts, R. E. Stratmann, O. Yazyev, A. J. Austin, R. Cammi, C. Pomelli, J. W. Ochterski, R. L. Martin, K. Morokuma, V. G. Zakrzewski, G. A. Voth, P. Salvador, J. J. Dannenberg, S. Dapprich, A. D. Daniels, O. Farkas, J. B. Foresman, J. V. Ortiz, J. Cioslowski, D. J. Fox, *Gaussian 09*, Revision C.01; Gaussian, Inc.: Wallingford, CT, **2010.**

[44] J. P. Perdew, K. Burke, M. Ernzerhof, *Phys. Rev. Lett.* **1996**, *77*, 3865-3868.

[45] a) K. Wolinski, J. F. Hinton, P. Pulay, *J. Am. Chem. Soc.* **1990**, *112*, 8251-8260; b) R. Ditchfield, *Mol. Phys.* **1974**, *27*, 789-807; c) F. London, *J. Phys. Radium* **1937**, *8*, 397-409.

[46] a) S. K. Wolff, T. Ziegler, E. van Lenthe, E. J. Baerends, *J. Chem. Phys.* **1999**, *110*, 7689-7698; b) S. K. Wolff, T. Ziegler, *J. Chem. Phys.* **1998**, *109*, 895-905; c) G. Schreckenbach, T. Ziegler, *Int. J. Quantum Chem.* **1997**, *61*, 899-918; d) G. Schreckenbach, T. Ziegler, *Int. J. Quantum Chem.* **1996**, *60*, 753-766; e) G. Schreckenbach, T. Ziegler, *J. Phys. Chem.* **1995**, *99*, 606-611.

[47] a) F. Weinhold, C. R. Landis, *Valency and bonding: A natural bond orbital donor acceptor perspective*; Cambridge University Press: Cambridge, U.K, **2005**; b) A. E. Reed, L. A. Curtiss, F. Weinhold, *Chem. Rev.* **1988**, *88*, 899-926.

[48] K. Wiberg, *Tetrahedron* **1968**, *24*, 1083-1096.

[49] Jmol: An Open-Source Java Viewer for Chemical Structures in 3D . http://www.jmol.org/

[50] T. Lu, F. Chen, *J. Comput. Chem.* **2012**, *33*, 580-592.

FULL PAPER

Synthesis of group 9 triple decker sandwich metallaheteroboranes containing four-membered open B_2E_2 central ring (E = S or Se) has been described. Further, the reactivity of these molecules with group 8 metal carbonyl compounds has been carried out that yielded *closo*-polyhedral metallaheteroboranes.

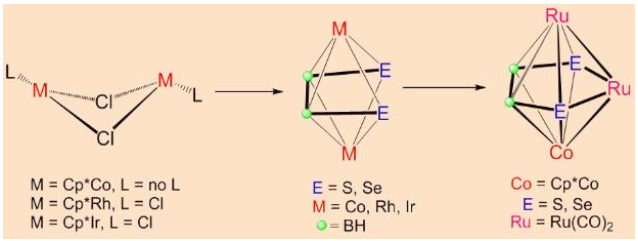

Benson Joseph,[a] Subrat Kumar Barik,†[a] Rongala Ramalakshmi,†[a] Gargi Kundu,[a] Thierry Roisnel,[b] Vincent Dorcet,[b] and Sundargopal Ghosh[a]*

Chemistry of Triple-Decker Sandwich Complexes Containing Four-Membered Open B_2E_2 Ring (E = S or Se)